Chaos Analysis of the Brain Topology in Grey Matter Images for the Recognition of Psychosis

Alexandra I. Korda (alexandra.korda@uksh.de)
Translational Psychiatry, Department of Psychiatry and Psychotherapy, University of Luebeck, Ratzeburger Allee 160, 23562 Luebeck

Mihai Avram
Translational Psychiatry, Department of Psychiatry and Psychotherapy, University of Luebeck, Ratzeburger Allee 160, 23562 Luebeck

Christina Andreou
Translational Psychiatry, Department of Psychiatry and Psychotherapy, University of Luebeck, Ratzeburger Allee 160, 23562 Luebeck

Thomas Martinetz
Institute for Neuro- and Bioinformatics, University of Luebeck, Germany, Ratzeburger Allee 160, 23562 Luebeck

Stefan Borgwardt
Translational Psychiatry, Department of Psychiatry and Psychotherapy, University of Luebeck, Ratzeburger Allee 160, 23562 Luebeck

Research Article

Keywords: First-episode psychosis, Clinical high risk, Brain sMRI, Biomarkers, Chaos analysis, Lyapunov exponent, Wavelet transformation, Gray matter topology

Posted Date: December 17th, 2021

DOI: https://doi.org/10.21203/rs.3.rs-1145694/v1

Abstract

Structural MRI studies in first-episode psychosis (FEP) and in clinical high risk (CHR) patients have consistently shown volumetric abnormalities in frontal, temporal, and cingulate cortex areas. The aim of the present study was to employ chaos analysis in the identification of people with psychosis. Structural MRI were acquired from 73 CHR, 77 FEP and 44 healthy controls (HC). Chaos analysis of the grey matter distribution was performed: first, the distances of each voxel from the center of mass in the grey matter image was calculated. Next, the distances multiplied by the voxel intensity was represented as a spatial-series, which then was analyzed by extracting the Largest-Lyapunov-Exponent (lambda). The lambda brain map depicts how the grey matter topology changes. The classification of a subject's clinical status was finally predicted by a) comparing the lambda brain maps, which resulted in statistically significant differences in FEP and CHR compared to HC; and b) matching the lambda series with the Morlet wavelet, which resulted in 100% accuracy in distinguishing between FEP and CHR. The proposed framework using spatial-series extraction enhances the classification decision for FEP, CHR and HC subjects, verifies diagnosis-relevant features and may potentially contribute to the identification of structural biomarkers for psychosis.

1. Introduction

Patterns of pathological alterations of the brain associated with illness emergence and progression have been a major interest of research in psychotic disorders [1]. Abnormalities in brain grey matter (GM) topology have been consistently observed in schizophrenia; these appear to be present already at the first-episode of psychosis (FEP) and even at subjects at clinical high risk (CHR) patients [2-8]. Abnormalities in cortical surface areas and cortical thickness have been consistently observed in schizophrenia as well. Drobinin et al. [9] reported that in youth at risk for mental illness displayed an overall trend toward lower cortical folding across all brain regions. Wisco et al. [10] compared cortical folding patterns between patients with schizophrenia and demographically matched healthy controls in prefrontal and temporal regions of interest. An area within the pars triangularis of the left inferior frontal gyrus (Broca's area) showed significantly reduced metric distortion in the patient group relative to the control group. Thinner cortex and smaller surface area in frontal and temporal lobe regions have been investigated in previous studies [11]. Neuroanatomical alterations in the medial prefrontal cortex and hippocampus were associated with abnormalities of the recognition of negative emotion at baseline in CHR patients [12]. In a case-control analysis [13], authors showed that schizophrenia was associated with increased heterogeneity in frontotemporal thickness and area and cortical, ventricle, and hippocampal volumes. In this study, we compare GM topology, including cortical surface, from GM images between FEP, CHR and HC subjects using the Largest-Lyapunov-Exponent. This metric implicates the geometry and curvature of all brain regions. Our aim was to analyze the chaotic dynamic of the GM topology and its usefulness for marking progression of the illness. To this extend, the scope of this study is to investigate the mechanism hidden in the GM topology on single-subject level.

Using three-dimensional magnetic resonance imaging and an analysis approach known from chaotic time series, we examined 73 CHR, 77 FEP patients and 44 HC. By transforming structural magnetic resonance imaging (sMRI) GM maps into spatial-series we compared the complexity of GM topology across the three groups. A spatial-series is the distribution of the weighted distance by voxel intensity from the GM centroid. The conversion of images into sequences for applications of time-series analysis tools has been utilized for solving several problems in image data mining [14]. As the GM morphology is inherently complex, chaos and nonlinear dynamics analyses of these spatial data are therefore suitable mathematical techniques for extracting their informative statistical properties. We introduce the term of GM topology for analysis of GM changes combining two features, each voxel's distance from the center of mass and each voxel's intensity. Chaos and nonlinear dynamics have been increasingly reported as effective computational methods for analyzing complex data in medicine and biology [15]. A previous study reported differences in complexity of brain folding in Alzheimer's disease and aging [16] by transforming sMRI images into spatial-series and comparing the Largest-Lyapunov-Exponent values in two groups. In this study, we explore the Largest-Lyapunov-Exponent (lambda) to determine the chaos and nonlinear dynamics of spatial-series data of GM topology in psychotic disorders. We focused on utilizing lambda as a descriptor that can quantify complexity of GM distribution in psychosis, with positive lambda values indicating chaos. Lambda is tackled here as a geometric shape descriptor of GM topology that considers subcortical areas in addition to surface characteristics. Continuous wavelet transformation is also applied in this study in order to have a useful representation of the spatial-scale of lambda for the proposed brain discrimination between FEP, CHR and HC.

The aim of the study is to employ chaos analysis for the identification of psychosis. We hypothesized that the nonlinear dynamics of brain topology in FEP and CHR is different from that of HC. It is not a group-level analysis but a single-subject level analysis that leads to 100% recognition of FEP and CHR subjects, while giving insights for the differentiation of CHR and FEP, respectively, from HC regarding the nonlinear dynamic of the GM topology.

2 Results

2.1 Localization

To perform localization, we transferred 5,000 lambda values extracted back to GM images. The lambda of voxels that were not selected as the top-weighted voxels is set to 0. The mean lambda map for FEP patients is presented in **Figure 1a)**, for CHR subjects in **Figure 1b)** and for HC subjects in **Figure 1c)**. As observed, common regions are captured in FEP and CHR subjects (e.g., frontal, temporal, and cingulate cortex areas, hippocampus, cerebellum and vermis). This fact supports our conclusion that identification of psychosis and clinical high risk can be performed using around 1% of GM voxels. The corrected FWE p-values are presented in Figure 2. Statistically significant differences were present in the occipital and temporal lobe for FEP and CHR compared to HC. No clusters were identified in between-group comparison results for CHR and FEP. The proposed method has low complexity, implements data

reduction, and leads to individual psychosis-stage recognition, by using the lambda maps of the 1% of the voxels, in approximately 1 hour using a high-performance computer.

2.2 Multi-scale analysis

In this study, 100 scales were selected after experimentation. As an example, in **Figure 3** the scalogram of one CHR subject, one FEP and one HC are presented. There are positive “matches” (correlation) and negative “matches” with the Morlet wavelet, as shown by the colorbar. Such scalograms can be used to better understand the dynamical behavior of a system and can also be used for distinguishing signals produced by different systems. Based on the multi-scale analysis, the brain spatial-series could be better understood and used for the identification of FEP and discrimination of FEP from CHR. In **Figure 3** the scalograms of one subject from each group are presented. Different patterns of FEP and CHR compared to HC are visible to the naked eye. 77 FEP patients present a common pattern such as the one shown in **Figure 3a)**, i.e., higher correlation with the Morlet wavelet in large scales between 40 and 80. 73 CHR subjects present a common pattern such as the one in **Figure 3b)**, i.e., higher correlation with the Morlet wavelet in scales between 20 and 80. 44 HC subjects present a common pattern such as the one in **Figure 3c)**, i.e., higher correlation with Morlet wavelet in large scales between 20 and 50.

T-tests for each scale were conducted with the significance level set at $p<0.05$, for the following group comparisons: i) FEP vs. HC, ii) FEP vs. CHR, and iii) CHR vs. HC. The scales and voxels that showed statistically significant differences (corrected with FDR<0.05) are presented in **Figure 4**. For the first comparison, scale 96 across voxels significantly differentiated FEP patients from HC. For comparison (ii), scales 94 and 96 across voxels significantly differentiated CHR from FEP patients. This indicates that low frequencies (high scales) presented in FEP express the sharp geometrical changes in the GM topology compared to CHR and HC. The identification of illness progression can be determined by looking at the scalograms in the scales indicated from the analysis. There was no statistically significant difference in the third comparison.

3. Discussion

In this study, grey matter abnormalities in the spatial-scale domain for a large sample of patients with first-episode psychosis (FEP), individuals’ clinical high risk (CHR) and healthy controls (HC) were investigated. We applied a combination of established methodologies using Largest-Lyapunov-Exponent and wavelet transformation to identify psychosis and CHR. The main advantage of the method is that it requires only 1% of the voxels in GM images for identification; in terms of low-complexity analysis, 5,000 voxels close to the surface of the GM centroid were sufficient for robust recognition of FEP and CHR.

We considered the nonlinear dynamics of the most weighted voxels by intensity and distance. Two outcome measures were used in this analysis: a) the lambda value and b) the scalograms. Lambda as an outcome measure successfully differentiated FEP and CHR patients from HC but was not sufficient to distinguish FEP from CHR. Multiple findings indicate similar brain abnormalities between CHR and FEP [2, 17-19]. Through localization of the top selected voxels and multiple comparisons of the lambda

across brain regions and groups, statistically significant differences were revealed in the occipital and temporal lobe and could serve as biomarkers of psychotic disorders. Many studies present the involvement of the occipital lobe in FEP and CHR [20-22]: Subjects with predominant attenuated psychotic symptoms are characterized by a reduction of GM-intensity values in the occipital cortex [22]. In previous studies in at-risk individuals progressive gray matter reductions in temporal regions were reported [23-25].

Our second outcome measure, scalograms of brain sMRI, were able to identify early-stage psychosis from CHR. Both FEP and CHR subjects could be differentiated from HC by simple visual inspection of the scalograms of the lambda extracted from the top 5,000 voxels. FEP scalograms were significantly different from those of HC and CHR; no differences were observed between CHR and HC. Thus, the move from the spatial domain into the frequency domain revealed hidden patterns in the mechanism of the progression of the disease. Two frequencies in the spatial-series of lambda provided the ability to statistically differentiate FEP from CHR, which was not possible using solely the lambda value. The small value of the frequencies presented by high scales was interpreted as sharp changes in the brain topology of FEP compared to CHR. We observed that the nonlinear dynamic of the weighted distances as an expression of the structure relief of the individual brains is highly informative for the identification of FEP and CHR subjects.

The innovation of the proposed method in the field of psychosis biomarker research is that it uses spatial-series extracted from sMRI, which separates it from other approaches that investigate grey matter volume increase or decrease, such as VBM analysis. Instead, our approach transforms the brain sMRI into a spatial-series, calculates the chaotic grey matter distribution using the lambda value, and finally transforms the lambda series into a two-dimensional (2D) scalogram by using the Wavelet Transform (WT), in order to have a useful representation of spatial-scale features.

The main advantage of the method is that the impact of the initial point of reference, the GM centroid in individual GM images, that was used for the calculation of the distance to voxels, is not reflected in the lambda value. Lambda measures how the distances diverge in the state-space, regarding the distances across all voxels selected, and thus is a ‘path-free’ measurement. As lambda expresses the way that two neighbor voxels, in the state-space, diverge across the GM topology with respect to all the other voxels, it depicts the way that voxels from different regions are related to structural changes in psychosis. As the scales represent the structure relief, it may reflect volume increase patterns in FEP patients compared to CHR subjects. However, our results should be considered in view of certain limitations: The sample size was moderate; moreover, the method contains many parameter selections that warrant further exploration (e.g., the number of the selected voxels). We plan to address these limitations in further studies investigating the effectiveness and robustness of the method in larger datasets with different scanning parameters, and across different (including non-psychotic) diagnoses.

4. Methods

4.1 Study participants

In this study, sMRI scans of 194 subjects were used, 73 CHR subjects, 77 FEP patients and 44 healthy controls (HC). Subjects were scanned using a SIEMENS MAGNETOM VISION 1.5T scanner (Erlangen, Germany) at the University Hospital Basel, Switzerland. The current analyses are based on data from patients included in the early detection of psychosis project (FePsy) at the Department of Psychiatry of the University of Basel [26] between November 2008 and April 2014. The study was approved by the local ethics committee of the University of Basel and written informed consent is obtained from each participant. The study was conducted in accordance with the Declaration of Helsinki.

A three-dimensional volumetric spoiled gradient recalled echo sequence generated 176 contiguous, 1-mm-thick sagittal slices. Imaging parameters were time-to-echo, 4ms; time-to-repetition, 9.7ms; flip angle, 12°; matrix size, 200 × 256; field of view, 25.6 × 25.6cm matrix; voxel dimensions, 1.28 × 1 × 1mm. Inclusion and exclusion criteria were described in [27]. For screening purposes, the Basel Screening Instrument for Psychosis (BSIP) was used, a 46-item instrument based on variables that have been shown to be risk factors or early symptoms of psychosis such as DSM-III-R – “prodromal symptoms,” social decline, drug abuse, previous psychiatric disorders, or genetic liability for psychosis [28].

4.2 MRI data processing

After inspection for artifacts and gross abnormalities, the T1-weighted images were segmented into grey matter (GM), white matter (WM), and cerebrospinal fluid (CSF) tissue maps in native space with the Cat12toolbox (http://dbm.neuro.uni-jena.de), an extension of the SPM12 software package (Wellcome Department of Cognitive Neurology, London, England). All scans were reviewed by a neuroradiologist to rule out clinically relevant abnormalities. Each participant’s GM, WM, and CSF maps were registered to stereotactic standard space. Next, for each subject, the modulated, warped, GM image (mwp1*) with an isotropic voxel size of 1.5 mm, was selected for the extraction of the spatial-series.

The command regionprops3 in MATLAB 2020b was used to get the centroid of the GM. To capture geometric changes in brain regions we calculated the weighted distance of the GM centroid with the voxel intensities. Reducing the computational costs, the weighted distances were sorted from the highest to lowest value. After experimentation, we concluded that the highest 5,000, expressing almost 1% of the non-zero voxels in the GM image, may be used for the identification of FEP and CHR patients. We ran the analysis using 1,000 to 5,000 voxels with a step of 1,000 voxels; significant results were identified selecting 5,000 voxels. We were interested in a method able to function under computational restrictions, which is why we chose only 1% of the voxels (5,000) for analysis. High weighted distances correspond to voxels that either belong to the cortical surface or close to the center of mass. For example, one point with intensity 1 and distance from the GM centroid 3 has the same weighted distance as one point with intensity 3 and distance 1. In Figure 5, a presentation of the mean weighted distance across every group for 500 voxels is shown. The measure was calculated with the same initial condition across subjects, starting from the same voxel and ends at the same voxels. Next, we analyzed the complexity of the brain topology to identify the stage of psychosis using the lambda and the wavelet transformation.

4.3 Largest Lyapunov Exponent

One of the most well-known method for quantitative measures of chaos is the Largest-Lyapunov-Exponent (lambda). A positive lambda expresses sensitive dependence on initial conditions for a dynamical system. A positive lambda presents the average rate over the whole attractor, at which two nearby trajectories become exponentially separate with time evolution [29]. A practical numerical technique for calculating lambda is the method developed by Rosenstein et al. [30], which works well with small datasets and is robust to changes in the embedding dimension, reconstruction delay, and noise level [31]. In brief, let x_i denote the spatial-series of the distances extracted from the brain sMRI. If it is assumed that the given spatial-series provides an observation of a dynamical system, then according to the theorem of Takens [31], the trajectory of the attractor of the system can be described by a matrix X. Each row, X_k, of the matrix is a state space vector:

$$X_k = \left[x_k, x_{k+\tau}, x_{k+2\tau}, \ldots, x_{k+(m-1)\tau}\right] \quad (1)$$

where $k = 0,1, \ldots, M-1$, $M = N-(m-1)\tau$, N is length of the spatial-series, τ and m are the embedding delay and the embedding dimension, respectively [32, 33].
After the state space reconstruction, the lambda can be defined using the following equation:

$$d(t) = d(0)\, e^{\lambda_1 t} \quad (2)$$

where λ_1 is the lambda value, $d(t)$ is the average divergence at the voxel t, and $d(0)$ is a constant that normalizes the initial separation.
Lambda can be estimated using the matrix X of the reconstructed state space as in [29]. A spatial-dependent value of lambda, $\lambda_1(k)$, where k the target voxel and T the distance between voxels in the state space, can be estimated as:

$$\lambda_1(k) = \frac{\langle lnd(k)\rangle - \langle lnd(k-1)\rangle}{T}, k > 1 \quad (3)$$

We performed a voxel-wise two-sample t-test in SPM12 for multiple comparisons (FWE<0.05) to compare the lambda value maps between a) FEP vs. HC, b) CHR vs. HC and c) FEP vs. CHR. FWE-corrected p-values are presented in **Figure 3**.

4.4 Wavelet transformation

Wavelet transform (WT) employs a fully scalable modulated window, which provides an extensively tested solution to the windowing function selection problem in frequency-related (scale-related) signal processing methodologies. The window slides across the signal, and for every position a spectrum is calculated. The procedure is then repeated at a multitude of scales, providing a signal representation with multiple spatial-scale resolutions. It does not only inform us about which scales are present in a signal, but also at which geometrical point these scales occur. This allows for good point resolution for high-

scale events, as well as good scale resolution for low-scale events, which is a combination of properties particularly well-suited for real signals. The rationale of the WT approach is that, firstly, the signal is “viewed” at a large scale/window and “large” features are analyzed and then the signal is “viewed” at smaller scales, in order to analyze “smaller” features.

In the present work continuous wavelet transform (CWT) was used for extracting features from lambda series obtained from the three types of groups that were described above. CWT was used to decompose the lambda series into their frequency components and the statistical features of the CWT coefficients were computed in the spatial domain. A CWT with a complex Morlet as mother function was used, see Figure 6. The WT of a 1-dimensional (1D) series has two dimensions. This 2-dimensional (2D) output of the WT provides the spatial-scale representation of the original series in the form of a “scalogram” plane. The two dimensions of a scalogram are the geometrical points and the scales. Each value (wavelet coefficient) in the scalogram plane represents the correlation of the lambda series with the Morlet wavelet on the respective point and scale pair.

Declarations

Author contributions

Alexandra I. Korda: Arise the research question, development of the proposed methodology, interpretation and writing of the results with the substantial help from all co-authors.

Mihai Avram: Preprocess of the MRI images.

Christina Andreou: MRI data acquisition, consultation on the interpretation of the results.

Stefan Borgwardt: MRI data acquisition, consultation on the interpretation of the results.

Thomas Martinetz: Consultation on the proposed methodology.

Competing Interests

The authors declare no competing interests.

References

1. Fornito, A., A. Zalesky, and M. Breakspear, *The connectomics of brain disorders.* Nature Reviews Neuroscience, 2015. **16**(3): p. 159-172.
2. Schmidt, A., et al., *Approaching a network connectivity-driven classification of the psychosis continuum: a selective review and suggestions for future research.* Frontiers in Human Neuroscience, 2015. **8**(1047).
3. Zhang, W., et al., *Brain gray matter network organization in psychotic disorders.* Neuropsychopharmacology, 2020. **45**(4): p. 666-674.

4. Fusar-Poli, P., et al., *Neuroanatomical Maps of Psychosis Onset: Voxel-wise Meta-Analysis of Antipsychotic-Naive VBM Studies.* Schizophrenia Bulletin, 2012. **38**(6): p. 1297-1307.
5. Brugger, S.P. and O.D. Howes, *Heterogeneity and Homogeneity of Regional Brain Structure in Schizophrenia: A Meta-analysis.* JAMA Psychiatry, 2017. **74**(11): p. 1104-1111.
6. Smieskova, R., et al., *Neuroimaging predictors of transition to psychosis—A systematic review and meta-analysis.* Neuroscience & Biobehavioral Reviews, 2010. **34**(8): p. 1207-1222.
7. Group, E.C.H.R.f.P.W., *Association of Structural Magnetic Resonance Imaging Measures With Psychosis Onset in Individuals at Clinical High Risk for Developing Psychosis: An ENIGMA Working Group Mega-analysis.* JAMA Psychiatry, 2021. **78**(7): p. 753-766.
8. Vissink, C.E., et al., *Structural brain volumes of individuals at clinical high risk for psychosis: a meta-analysis.* Biological Psychiatry Global Open Science, 2021.
9. Drobinin, V., et al., *Psychotic symptoms are associated with lower cortical folding in youth at risk for mental illness.* Journal of Psychiatry and Neuroscience, 2020. **45**(2): p. 125-133.
10. Wisco, J.J., et al., *Abnormal cortical folding patterns within Broca's area in schizophrenia: evidence from structural MRI.* Schizophrenia research, 2007. **94**(1-3): p. 317-327.
11. van Erp, T.G.M., et al., *Cortical Brain Abnormalities in 4474 Individuals With Schizophrenia and 5098 Control Subjects via the Enhancing Neuro Imaging Genetics Through Meta Analysis (ENIGMA) Consortium.* Biological psychiatry, 2018. **84**(9): p. 644-654.
12. Modinos, G., et al., *Association of Adverse Outcomes With Emotion Processing and Its Neural Substrate in Individuals at Clinical High Risk for Psychosis.* JAMA Psychiatry, 2020. **77**(2): p. 190-200.
13. Alnæs, D., et al., *Brain Heterogeneity in Schizophrenia and Its Association With Polygenic Risk.* JAMA Psychiatry, 2019. **76**(7): p. 739-748.
14. Yoon-Sik, T. and H. Eenjun. *A Leaf Image Retrieval Scheme Based on Partial Dynamic Time Warping and Two-Level Filtering*. in *7th IEEE International Conference on Computer and Information Technology (CIT 2007)*. 2007.
15. Pham, T.D., et al., *Measures of Morphological Complexity of Gray Matter on Magnetic Resonance Imaging for Control Age Grouping.* Entropy, 2015. **17**(12).
16. Chen, Y. and T.D. Pham, *Sample entropy and regularity dimension in complexity analysis of cortical surface structure in early Alzheimer's disease and aging.* Journal of Neuroscience Methods, 2013. **215**(2): p. 210-217.
17. Fusar-Poli, P., et al., *The Psychosis High-Risk State: A Comprehensive State-of-the-Art Review.* JAMA Psychiatry, 2013. **70**(1): p. 107-120.
18. Fusar-Poli, P., et al., *Heterogeneity of Psychosis Risk Within Individuals at Clinical High Risk: A Meta-analytical Stratification.* JAMA Psychiatry, 2016. **73**(2): p. 113-120.
19. Bykowsky, O., et al., *Association of antidepressants with brain morphology in early stages of psychosis: an imaging genomics approach.* Scientific Reports, 2019. **9**(1): p. 8516.

20. Koutsouleris, N., et al., *Use of Neuroanatomical Pattern Classification to Identify Subjects in At-Risk Mental States of Psychosis and Predict Disease Transition.* Archives of General Psychiatry, 2009. **66**(7): p. 700-712.
21. Tohid, H., M. Faizan, and U. Faizan, *Alterations of the occipital lobe in schizophrenia.* Neurosciences (Riyadh, Saudi Arabia), 2015. **20**(3): p. 213-224.
22. Zikidi, K., et al., *Grey-matter abnormalities in clinical high-risk participants for psychosis.* Schizophrenia Research, 2020. **226**: p. 120-128.
23. Borgwardt, S.J., et al., *Regional Gray Matter Volume Abnormalities in the At Risk Mental State.* Biological Psychiatry, 2007. **61**(10): p. 1148-1156.
24. Chung, Y., et al., *Cortical abnormalities in youth at clinical high-risk for psychosis: Findings from the NAPLS2 cohort.* NeuroImage: Clinical, 2019. **23**: p. 101862.
25. Takahashi, T., et al., *Progressive Gray Matter Reduction of the Superior Temporal Gyrus During Transition to Psychosis.* Archives of General Psychiatry, 2009. **66**(4): p. 366-376.
26. Riecher-Rössler, A., et al., *The Basel early-detection-of-psychosis (FEPSY)-study – design and preliminary results.* Acta Psychiatrica Scandinavica, 2007. **115**(2): p. 114-125.
27. Borgwardt, S., et al., *Distinguishing prodromal from first-episode psychosis using neuroanatomical single-subject pattern recognition.* Schizophrenia bulletin, 2013. **39**(5): p. 1105-1114.
28. Riecher-Rössler, A., et al., *Das Basel Screening Instrument für Psychosen (BSIP): Entwicklung, Aufbau, Reliabilität und Validität.* Fortschr Neurol Psychiatr, 2008. **76**(04): p. 207-216.
29. Korda, A.I., et al., *Automatic identification of eye movements using the largest lyapunov exponent.* Biomedical Signal Processing and Control, 2018. **41**: p. 10-20.
30. Rosenstein, M.T., J.J. Collins, and C.J. De Luca, *A practical method for calculating largest Lyapunov exponents from small data sets.* Physica D: Nonlinear Phenomena, 1993. **65**(1): p. 117-134.
31. Takens, F. *Detecting strange attractors in turbulence*. in *Dynamical Systems and Turbulence, Warwick 1980*. 1981. Berlin, Heidelberg: Springer Berlin Heidelberg.
32. Strogatz, S.H., *Nonlinear Dynamics and Chaos: With Applications to Physics, Biology, Chemistry, and Engineering (2nd ed.).* , ed. C. Press. 2015.
33. Kennel, M.B., R. Brown, and H.D.I. Abarbanel, *Determining embedding dimension for phase-space reconstruction using a geometrical construction.* Physical Review A, 1992. **45**(6): p. 3403-3411.

Figures

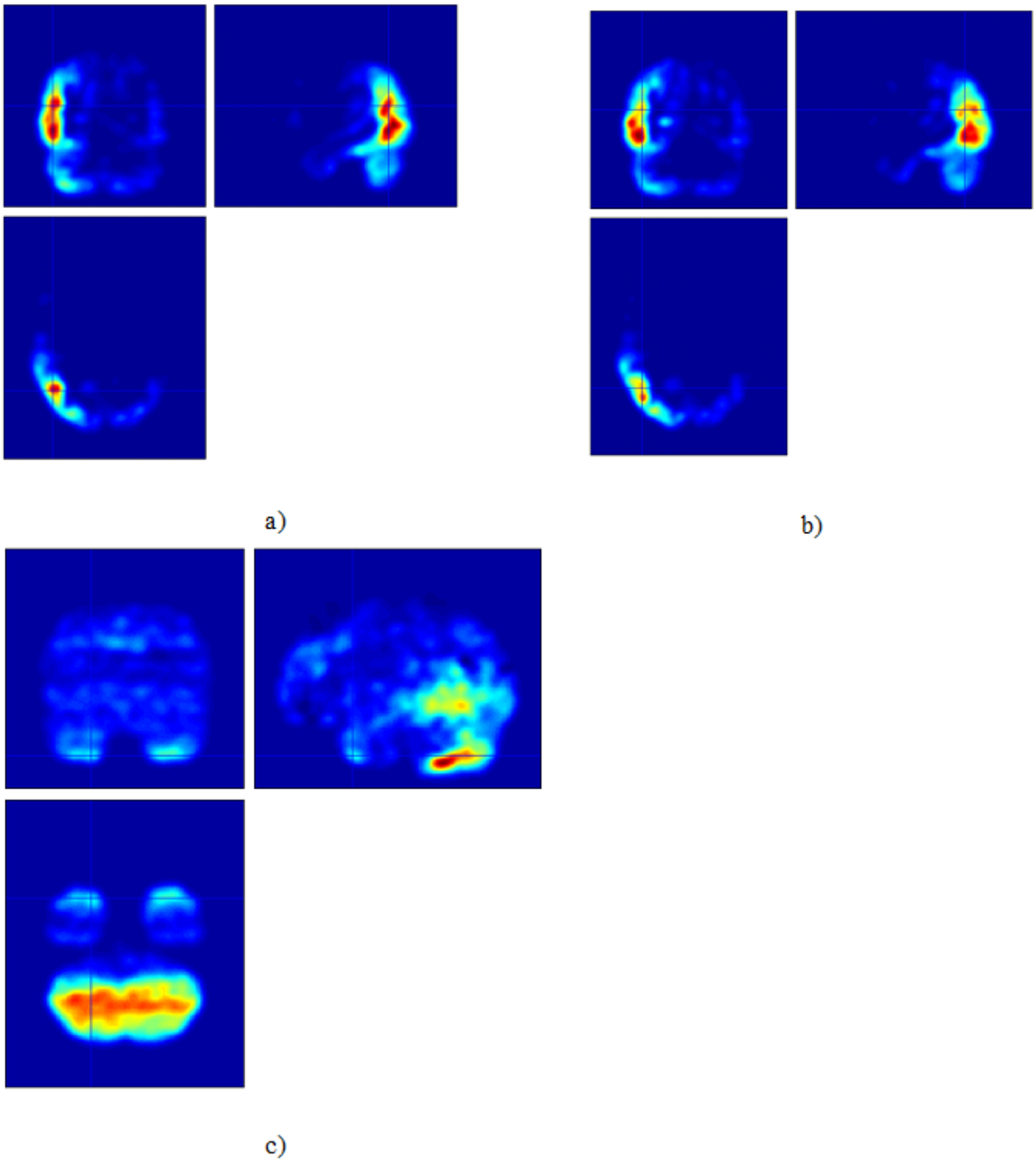

Figure 1

Representation of the mean lambda map of the top weighted distances in a) FEP, b) CHR and c) HC in the MNI space using the SPM12 toolbox.

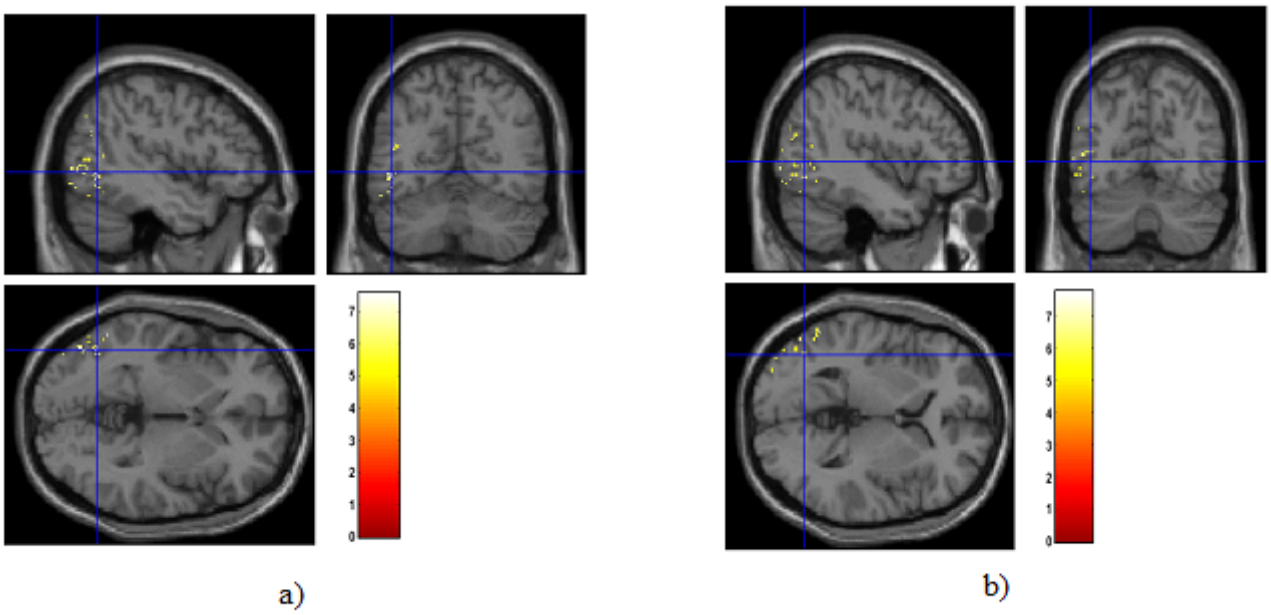

Figure 2

Visualization of between-group comparison results. Corrected p-values (FWE<0.05) in a) FEP vs. HC, and b) CHR vs. HC.

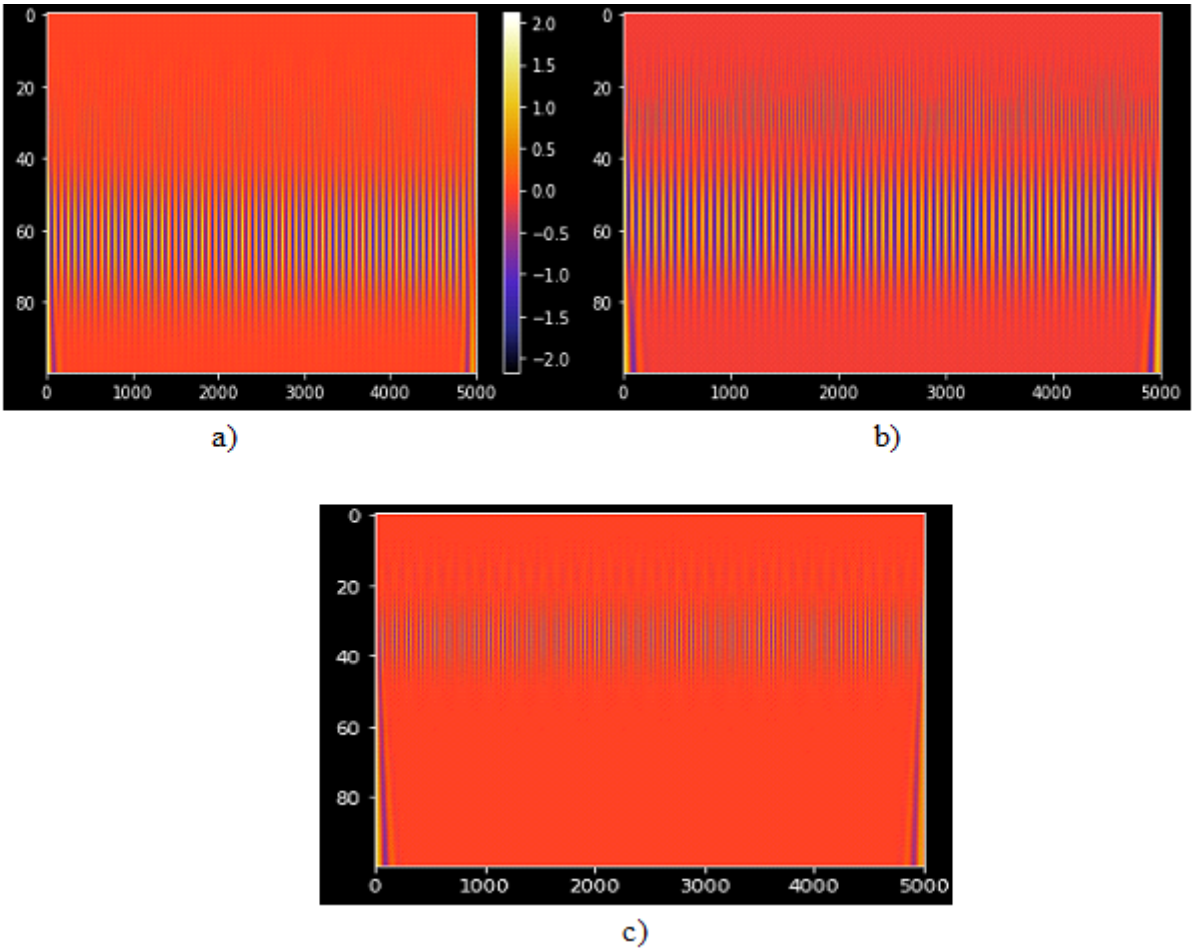

Figure 3

Scalogram of one a) FEP, b) CHR and c) HC subject. Voxels are represented in x-axis and scales in y-axis.

Figure 4

Statistically significant differences, corrected with FDR<0.05, between groups a) FEP vs. HC and b) FEP vs. CHR.

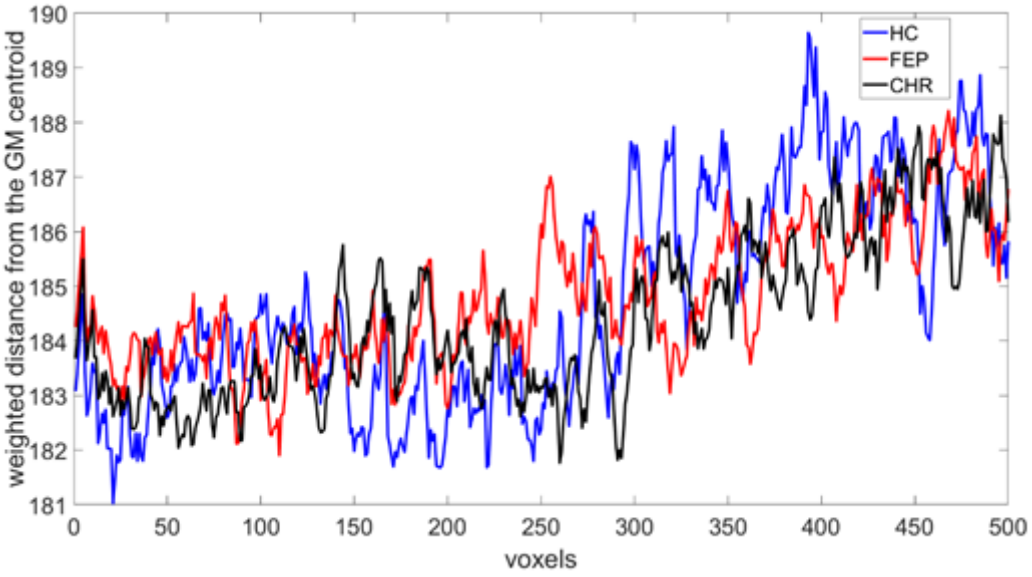

Figure 5

Weighted distance from the GM centroid and voxels, extracted from HC, CHR and FEP group.

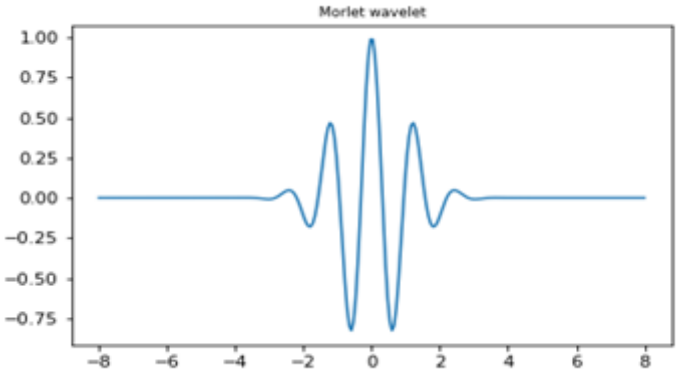

Figure 6

Morlet wavelet